

A SHAPE ANALYSIS OF ULTRASONICALLY LEVITATED DROPLET WITH MOVING PARTICLE SEMI-IMPLICIT AND DISTRIBUTED POINT SOURCE METHOD

YUJI WADA*, KOHEI YUGE*, RYOHEI NAKAMURA[†], HIROKI TANAKA[†] AND KENTARO NAKAMURA[†]

* Faculty of Science and Technology, Seikei University, 3-3-1 Kichijoji-kitamachi, Musashino-shi, Tokyo 180-8633, Japan
e-mail: yuji.wada@st.seikei.ac.jp

[†]Precision and Intelligence Laboratory, Tokyo Institute of Technology, 4259-R2-26 Nagatsutacho, Midori-ku, Yokohama, 226-8503 Japan

Key words: Acoustic Radiation Force, Particle Method, Point Source Method, Surface Tension, Ultrasonic levitation

Abstract. Ultrasonic droplet levitation has recently been drawing attention as a way of non-contact transportation. Many experiment revealed that levitating droplet changes its shape to spheroid, however, quite small number of numerical simulation have discussed this phenomenon including fluid dynamics within the droplet. In this paper, the coupled analysis using distributed point source method (DPSM) and moving particle semi-implicit (MPS) method is suggested, both of which does not require grids or meshes, therefore, can handle the moving boundary with ease. The levitating ultrasonic droplet in plane standing wave field between the ultrasonic transducer and the reflector is simulated with the DPSM-MPS coupled method. The spheroidal droplets are successfully reproduced numerically, and ratio of the change in spheroidal ratio and the gravitational center position are discussed.

1 INTRODUCTION

Ultrasonic levitation has recently been drawing attention as a way of non-contact transportation of small objects, such as liquid droplets, in bioengineering and manufacturing industry[1]. The small objects in the finite amplitude sound field have been known to be trapped near the pressure node of the standing wave with the effect of acoustic radiation force[2, 3, 4]. Many experimental reports are presented related to the droplet levitation[5, 6, 7, 8, 9] and their shape in the air[10, 11, 12]. The droplet with large volume is reported to turn its shape from sphere to spheroid when they are exposed

in the intense sound pressure field[11]. Several analytical reports have mentioned this phenomenon[13, 14], however, almost no report carried out dynamical simulation on the shape change of the droplet.

In this paper, the levitated droplet shape is simulated by coupling two gridless analysis methods, the one is distributed point source method (DPSM[15, 16, 17, 18]) and the other is moving particle semi-implicit (MPS[19, 20]) method.

2 LEVITATION BY ACOUSTIC RADIATION

The static pressure under finite amplitude sound, acoustic radiation pressure P_a , is known to appear as a result of acoustic nonlinearity[2, 3, 4]. The magnitude of the static pressure is expressed to be the difference between the time averaged potential energy $\langle e_p \rangle$ and kinetic energy $\langle e_k \rangle$ as

$$P_a = \langle e_p \rangle - \langle e_k \rangle, = \frac{\langle p^2 \rangle}{2\rho c^2} - \frac{\rho \langle \mathbf{u}^2 \rangle}{2}, \quad (1)$$

where p , \mathbf{u} and ρ is sound pressure, sound particle velocity, density of acoustic medium and $\langle \dots \rangle$ means the operation of time average, respectively. The surface integral on the droplet produces the acoustic radiation force as

$$\mathbf{F}_a = \iint P_a \mathbf{n} dS, \quad (2)$$

where \mathbf{n} is the normal unit vector to the droplet surface.

Figure 1 shows the overview about the forces acting on the droplet, levitating near the pressure node in the plane standing wave field along vertical axis. Gravity and surface tension as well as acoustic radiation force is assumed in such case.

Acoustic radiation pressure is positive on the upper and lower surface of the droplet, because the most of kinetic energy in eq.(1) is interfered by the great difference of acoustic impedance between air and liquids. When the lower acoustic radiation force balances the sum of the upper radiation force and gravity, the droplet can remain in the air often just below the pressure node.

For the horizontal balance of the force, acoustic radiation pressure is negative on the side surface of the droplet, because the kinetic energy is not interfered by droplet surface and the sound pressure potential energy is small at the pressure node. This acoustic radiation force stretches the side surface of the droplet to spheroid, while the surface tension act against it for the increase in the surface curvature.

However, the droplet shape cannot be determined from single sound field analysis, because the sound field will be changed by the acoustic scattering with the new droplet shape. To derive the true droplet shape, an iterative coupled analysis of sound field and incompressible fluid dynamics is required, where the droplet shape and the acoustic radiation pressure are exchanged.

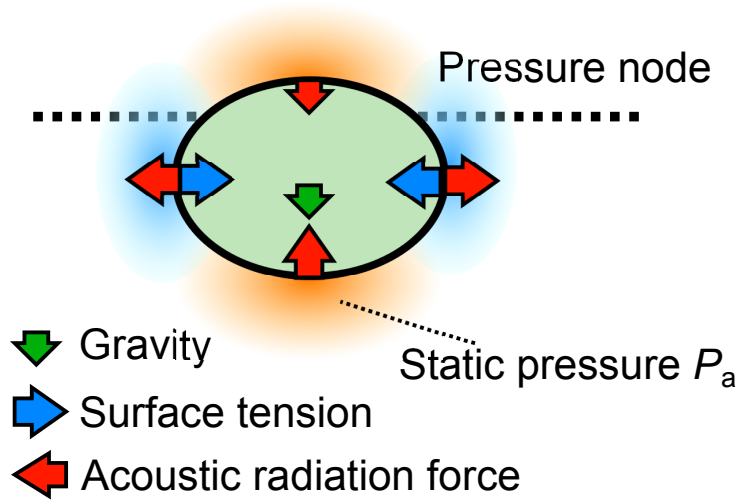


Figure 1: Forces act on an ultrasonic levitated droplet.

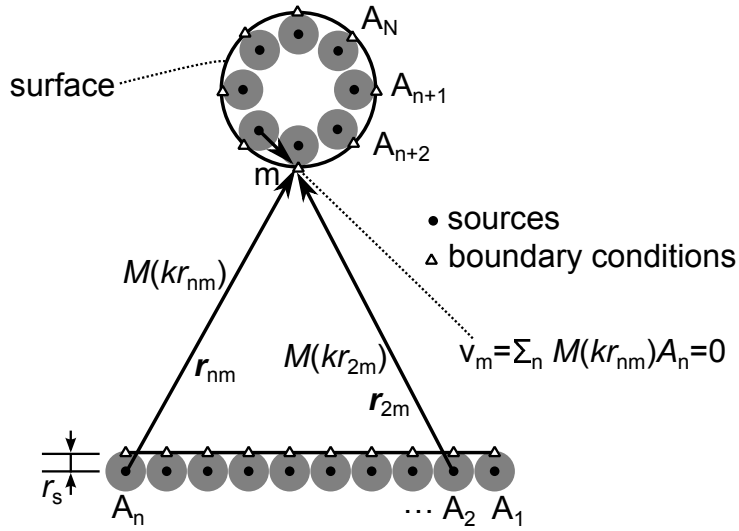
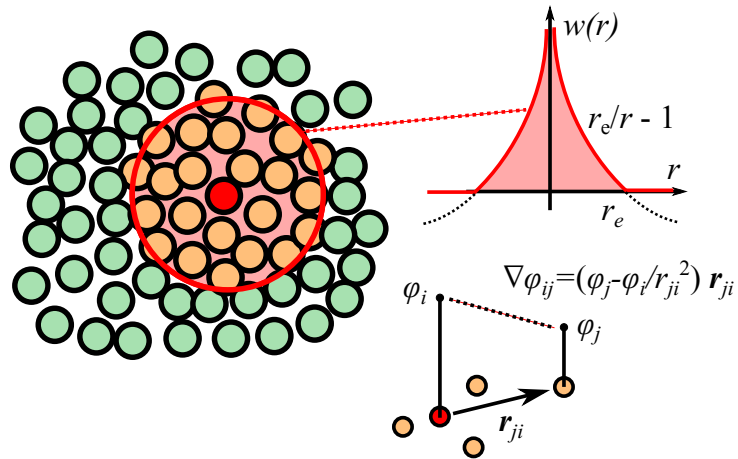


Figure 2: Distributed point sources and boundary conditions.



3
Figure 3: Moving particle semi-implicit method window and gradient.

3 DISTRIBUTED POINT SOURCE METHOD

DPSM[15, 16, 17, 18] is a sound field analysis method which does not requires calculation grids or meshes, but distributed sphere sound sources. Since DPSM requires no element-node connectivity, the calculation routine can spare troublesome mesh regeneration or any extra conservation treatment.

DPSM is based on Huygens-Fresnel superposition principle and Rayleigh-Sommerfeld integral [21]. The sound field p from a vibrator with known vibration velocity V is calculated with area integral. Numerically, this integral can be regarded to be the summation of the product of the complex number source \mathbf{A} and Green functions $G(kr)$.

$$p = \frac{j\omega\rho}{2\pi} \iint V G(kr) dS \simeq \sum_n^N G(kr) \{A_n\}, \quad (3)$$

$$A_n = \frac{j\omega\rho}{2\pi} V \Delta S, \quad G(kr) = \frac{e^{-jkr}}{r}, \quad (4)$$

where ω , k and r is angular ultrasonic frequency, wavenumber and the distance from the source to the target, respectively.

DPSM can model reflecting boundary and interface as well as transmitting interface in the following manner. Figure 2 shows the schematic diagram of DPSM. Point sources with unknown amplitude A are placed slightly behind the boundary or interface at the centers of imaginary small spheres with radius r_s . These spheres touch the boundary surface or interface on a point m . Therefore, the distance between the point sources and the boundary or interface is equal to the sphere radius. Sound pressure and particle velocity along the vector \mathbf{n} at the point m have following relationship with the unknown sources \mathbf{A} .

$$p_m = \sum_n^N G(r_{mn}) A_n \quad (5)$$

$$v_m = - \sum_n^N \frac{\mathbf{n} \cdot \mathbf{r}_{mn}}{j\omega\rho} \frac{\partial p}{\partial r} = \sum_n^N M(r_{mn}) A_n \quad (6)$$

If a source belong to the vibrator or the reflector, v_m is set to be V_0 or 0 as a boundary condition, respectively. Now that N boundary condition is specified for N unknown sources, the amplitude of the point sources are calculated by satisfying all boundary and interface conditions.

$$\{A_n\} = [M_{mn}]^{-1} \{V_m\} \quad (7)$$

$$\{V_m\} = {}^t \{V_0, \dots, V_0, 0, \dots, 0\} \quad (8)$$

After determining the source amplitude, sound pressure and particle velocity at droplet surface can be obtained. Then, the acoustic radiation pressure P_a is calculated with eq.(1).

4 MOVING PARTICLE SEMI-IMPLICIT

Particle method is one of the way to calculate the fluid dynamics without any grid of mesh. It treats the fluid motion not in Eulerian form but Lagrangian form and calculates the motion of fluid by distributed particles. MPS method [19, 20] is one of such particle method. Figure 3 shows the schematic diagram of MPS method. The spatial differential of a certain variable ϕ on the particle i is calculated in following equation.

$$\nabla\phi_i = \frac{D}{d^0} \sum_{j \neq i} \left[\frac{\phi_j - \phi_i}{r_{ji}^2} \mathbf{r}_{ji} w(r_{ji}) \right], \quad (9)$$

where D and d^0 are dimension number and initial particle density, respectively. The weighting function and the particle density are calculated as

$$w(r) = \begin{cases} r_e/r - 1 & (0 < r \leq r_e) \\ 0 & (r > r_e) \end{cases}, \quad (10)$$

$$d_i = \sum_{j \neq i} w(r_{ji}), \quad (11)$$

where r_e is the influence radius of MPS.

Equation (12) indicates the incompressible fluid equation in Lagrangian form, which is handled in MPS.

$$\frac{\partial U}{\partial t} = -\frac{\nabla(P + \sigma\kappa + P_a)}{\rho_w} + \nu\nabla^2 U + g, \quad (12)$$

where ρ_w, g, σ and κ are density of the droplet liquid, gravity, surface tension constant and curvature of the surface, respectively.

Simplified marker and cell (SMAC) algorithm is applied to the MPS method, and the pressure is calculated from Poisson equation as

$$\nabla P^2 = \frac{\rho_w}{\Delta t} \text{div } U. \quad (13)$$

The surface tension and the acoustic radiation pressure is input as a boundary condition of Poisson equation.

5 SURFACE DETECTION AND SURFACE TENSION

The surface particle is detected by threshold the ration of the current particle density by initial density, that is, if $d_i < \beta d^0$, the particle i is surface particle[19].

The unit normal vector of the edge particle i is calculated from the MPS-weight averaged position vector \mathbf{r}_{ij} as

$$\mathbf{n}_i = \frac{\sum_{j \neq i} \mathbf{r}_{ji} w(r_{ji})}{\left| \sum_{j \neq i} \mathbf{r}_{ji} w(r_{ji}) \right|}. \quad (14)$$

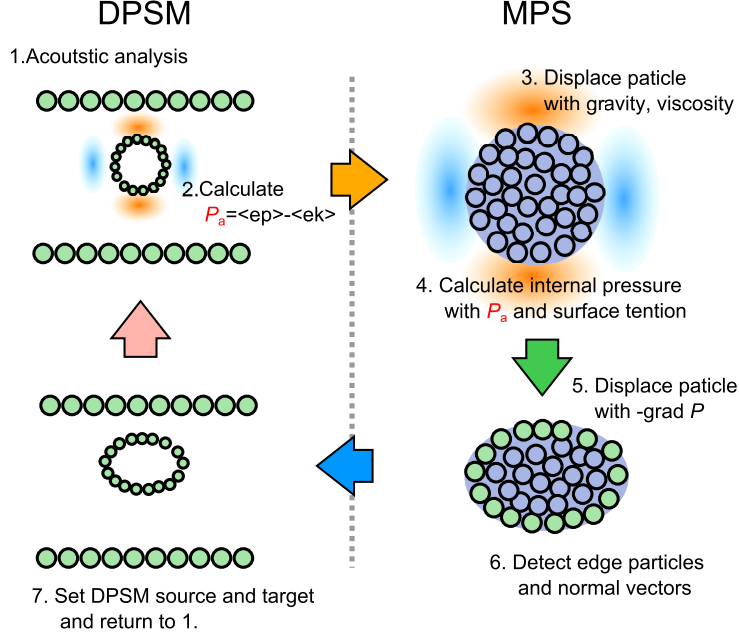


Figure 4: Calculation procedure for DPSM-MPS interaction analysis.

The surface particle is treated as a sphere source in DPSM routine, and the DPSM boundary condition point is located at $(\mathbf{r}_i + r_s \mathbf{n})$.

The curvature κ , which is required for the input the surface tension, is calculated from the position vector \mathbf{r}_{ij} , the normal unit vector \mathbf{n} as and the tangent unit vector \mathbf{l} by predicting function curvature with $(\partial^2 n / \partial l)$.

$$\kappa_i = \frac{\sum_{(j \in \Gamma) \neq i} 2 \frac{(\mathbf{r}_{ji} \cdot \mathbf{n})}{(\mathbf{r}_{ji} \cdot \mathbf{l})^2} w(r_{ij})}{\sum_{(j \in \Gamma) \neq i} w(r_{ij})} \quad (15)$$

$$\mathbf{l} = \mathbf{n} \times (\mathbf{n} \times \mathbf{r}_{ji}) / r_{ji}, \quad (16)$$

where Γ is the set of edge particle.

Figure 4 shows the flowchart of the DPSM-MPS coupled analysis. The coupling calculation proceeds with the exchange of the acoustic radiation force and the droplet surface particle locations.

6 CALCULATION PROBLEM

Figure 5 indicates the problem geometry and material properties for the ultrasonic droplet levitation. The droplet is levitated in the plane standing wave field with two acoustic node plane, which is excited between the bolt-cramped Langevin transducer with

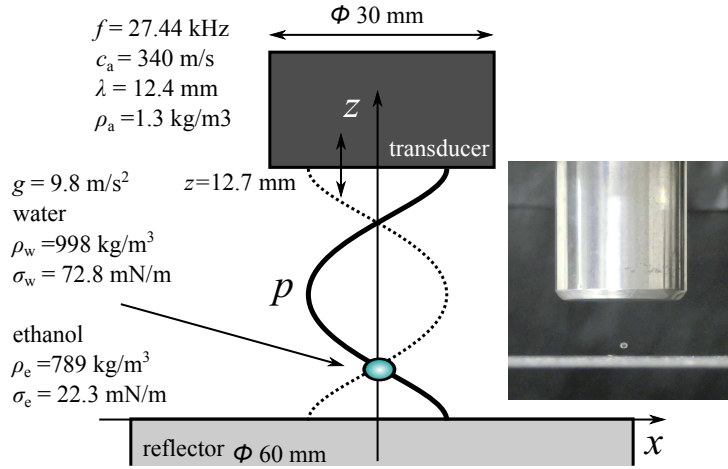


Figure 5: Problem geometry for an ultrasonic levitated droplet.

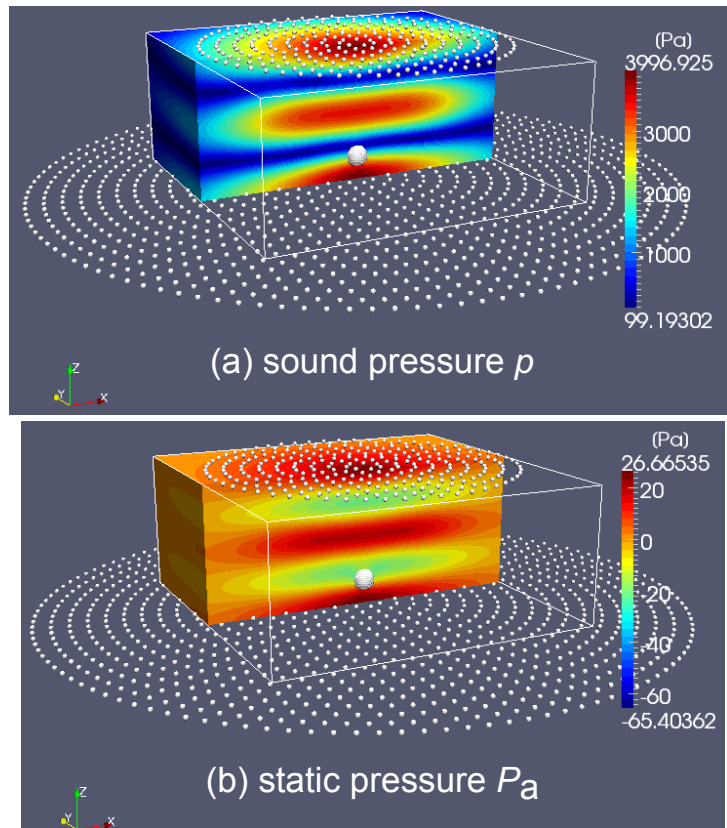


Figure 6: (a) Sound pressure and (b) static pressure distribution with initial radius of $\lambda/40$, where the black and white spheres are DPSM boundary condition point and DPSM source, respectively.

stepped horn and the plane reflector. The ultrasonic frequency, vibration amplitude and surface radius of the horn are 27.44 kHz, 0.5 m/s in zero-to-peak and 15 mm, respectively.

The medium of the droplet is water and ethanol, and the initial radius of the droplet is 0.4, 0.6, 0.8 and 0.9 mm. The droplet is levitated near the lower node of the standing wave field, which is located at $z = 3.1$ mm, quarter-wavelength above the reflector. The initial position of the droplet is set to be $z = 2.2$ mm.

For MPS parameters, initial particle placement interval dr is set to be one-eighth of the droplet radius. The influence radius r_e is $4dr$. For the convergence of the calculation, 100 times larger viscosity, $\nu = 100$ cSt is applied. And air resistance proportional to velocity with $(0.01/dt)$ [s^{-1}] is also applied. MPS transient time interval and calculation time are $dt=50 \mu s$ and 30 ms (600 steps), respectively.

For DPSM parameters, the radius of point source is dr on the droplet and $\lambda/8$ on the vibrator and the reflector. For ease in handling, the surface of the droplet is treated as acoustically rigid. For the fast calculation, DPSM calculation is done for every 20 steps according with MPS calculation.

7 RESULTS AND DISCUSSION

Figure 6 shows the sound pressure and the radiation pressure distribution on the initial time step. The white spheres in the figure indicate the DPSM sound source, and spread out on the vibration, reflector, droplet surface. The amplitude of the sound pressure is 4 kPa at the antinode of the standing wave, and the radiation pressure has + 27 and -65 Pa on vertical and side surface of the droplet, respectively.

Figure 7 shows the droplet deformation and radiation pressure at the time 0, 2, 5 and 30 ms. The droplet levitates because the vertical positive static pressure balances the gravity, and the shape turns into spheroid because the horizontal negative static pressure balances the surface tension. The change in shape completes in several milliseconds, and after that the droplet is observed to move toward the node.

Figure 8 shows the transient response of the gravitational center position for the water and ethanol droplet with radius from 0.4 to 0.9. Final levitation position is settled at $z=2.9$ mm, which is 0.2 mm below the pressure node. The ethanol droplets move towards the pressure nodes 10 % faster than the water droplets. This is attributed to the mass of liquid, where the density of ethanol is almost 20 smaller than that of water, and the radiation pressure is not dependent on liquids. Then, the ethanol droplets have smaller inertia than water droplets, therefore, the ethanol droplets have larger acceleration than the water droplets. Note that the larger air resistance is applied in this analysis, the actual velocity would be faster than these calculations.

Figure 9 shows the temporal change of the horizontal-vertical spheroid ratio. The droplets with larger initial radius tend to change its shape flatter than smaller ones asking for larger curvature to balance the negative radiation pressure. The ethanol droplet has approximately 1.5 times flatter than the water droplet with the same initial radius. This is attributed to surface tension constant of ethanol is one-third of that of water, therefore,

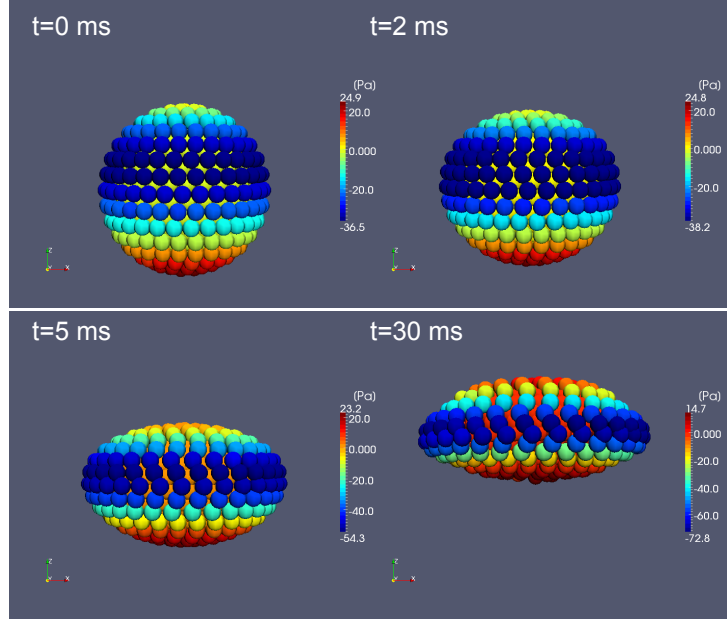


Figure 7: Ethanol droplet deformation and internal pressure at the time 0, 0.5, 2, 20 ms with initial radius of $\lambda/40$.

the ethanol droplets changed its shape asking for larger curvature.

8 CONCLUSIONS

The shape of an ultrasonic levitated droplet was simulated using MPS and DPSM in three dimensional space to confirm the experimentally well-known fact that the droplet shape turns to spheroid. As a result, by the acoustic radiation pressure, the droplet turned to spheroid and the droplet has settled down to just below the pressure node. The change rate of gravitational center position and spheroid ratio is different depending on the droplet medium.

For future study, the comparison to the measurement or literature data, and non-statical movement of the droplet, such as flow within the droplet or on the droplet surface, or process of droplet breaking up, is needed to consider.

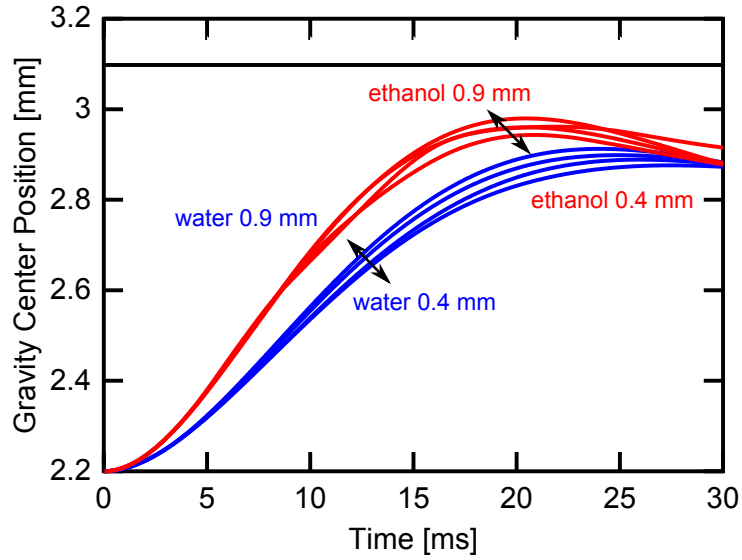


Figure 8: Time variation of the gravity center position of the droplet with various initial radii.

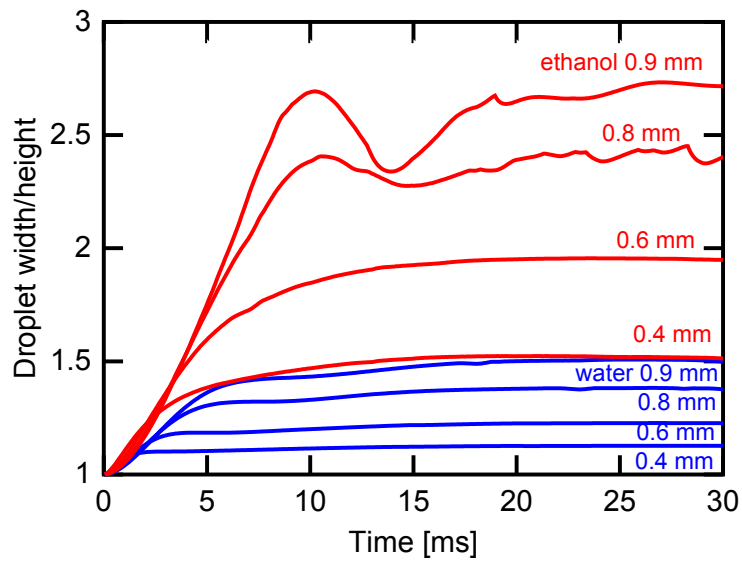


Figure 9: Time variation of the ratio of width to height of the droplet with various initial radii.

REFERENCES

- [1] J. Friend, L. Y. Yeo, Microscale acoustofluidics: Microfluidics driven via acoustics and ultrasonics, *Rev. Mod. Phys.* 83 (2011) 647–704.
- [2] L. V. King, On the acoustic radiation pressure on spheres, *Philos. Trans. R. Soc. London, Ser. A* 147 (861) (1934) 212–240.
- [3] W. L. Nyborg, Radiation pressure on a small rigid sphere, *J. Acoust. Soc. Am.* 42 (5) (1967) 947–952.
- [4] Z. A. Gol'dberg, *High-Intensity Ultrasonic Fields*, Plenum Publishing Corporation, 1971, Ch. 2.
- [5] R. Whymark, Acoustic field positioning for containerless processing, *Ultrasonics* 13 (6) (1975) 251 – 261.
- [6] T. Otsuka, T. Nakane, Ultrasonic levitation for liquid droplet, *Jpn. J. Appl. Phys.* 41 (Part 1, No. 5B) (2002) 3259–3260.
- [7] M. Ding, D. Koyama, K. Nakamura, Noncontact ultrasonic transport of liquid using a flexural vibration plate, *Applied Physics Express* 5 (9) (2012) 097301.
- [8] H. Tanaka, Y. Wada, Y. Mizuno, K. Nakamura, Behavior of ultrasonically levitated object above reflector hole, *Jpn. J. Appl. Phys.* 52 (2013) 100201.
- [9] R. Nakamura, Y. Mizuno, K. Nakamura, Demonstration of noncontact ultrasonic mixing of droplets, *Jpn. J. Appl. Phys.* 52 (2013) 07HE02.
- [10] P. L. Marston, R. E. Apfel, Quadrupole resonance of drops driven by modulated acoustic radiation pressure experimental properties, *J. Acoust. Soc. Am.* 67 (1) (1980) 27–37.
- [11] Y. Abe, M. Kawaji, T. Watanabe, Study on the bubble motion control by ultrasonic wave, *Exp. Therm. and Fluid Sci.* 26 (67) (2002) 817 – 826.
- [12] Y. Yamamoto, Y. Abe, A. Fujiwara, K. Hasegawa, K. Aoki, Internal flow of acoustically levitated droplet, *Microgravity Science and Technology* 20 (3-4) (2008) 277–280.
- [13] A. L. YARIN, M. PFAFFENLEHNER, C. TROPEA, On the acoustic levitation of droplets, *Journal of Fluid Mechanics* 356 (1998) 65–91.
- [14] I. Murray, S. Heister, On a droplet's response to acoustic excitation, *International Journal of Multiphase Flow* 25 (3) (1999) 531 – 550.
- [15] D. Placko, T. Kundu (Eds.), *DPSM for Modeling Engineering Problems*, 1st Edition, Wiley-Interscience, 2007, p. 372.

- [16] T. Kundu (Ed.), *Ultrasonic Nondestructive Evaluation: Engineering and Biological Material Characterization*, 1st Edition, CRC Press, 2004, p. 848.
- [17] T. Kundu, D. Placko, E. Rahani, T. Yanagita, C. M. Dao, Ultrasonic field modeling: a comparison of analytical, semi-analytical, and numerical techniques, *IEEE Trans. Ultrason. Ferroelectr. Freq. Control* 57 (12) (2010) 2795–2807.
- [18] T. Kundu, D. Placko, T. B. S. Das, E. K. Rahani, *Ultrasonic and Electromagnetic NDE for Structure and Material Characterization: Engineering and Biomedical Applications*, CRC Press, 2012, Ch. 2: Modeling of Ultrasonic Fields by Distributed Point Source Method (DPSM), pp. 109–168.
- [19] S. Koshizuka, Y. Oka, Moving-particle semi-implicit method for fragmentation of incompressible fluid, *Nucl. Sci. Eng.* 123 (1996) 421–434.
- [20] S. Koshizuka, A. Nobe, Y. Oka, Numerical analysis of breaking waves using the moving particle semi-implicit method, *International Journal for Numerical Methods in Fluids* 26 (7) (1998) 751–769.
- [21] J. W. S. Rayleigh, *Theory of Sound*, Vol. 2, Dover, New York, 1945, pp. 192–169.